AA bilayer coupler

Petr Červenka[1]

[1]Department of Physics, Faculty of Nuclear Sciences and Physical Engineering, Czech Technical University in Prague
cervep12@cvut.cz

Abstract

Two non-interacting graphene sheets are deformed in a localized region where they form AA bilayer graphene. This theoretical model is called the AA bilayer coupler. We show that the Hamiltonian of this system can be elegantly block-diagonalized. On the coupler, the scattering properties of Dirac fermions in two dimensions are analyzed through a partial wave decomposition. The differential and partial cross sections reveal some interesting phenomena, such as pouring particles from one layer to the other, filtering Dirac fermions with a given value of angular momentum, or the formation of quasi-bound states.

Keywords: AA bilayer graphene; Dirac equation; scattering, solvable models.

Introduction

Rapid scientific progress in the field of 2D materials demands a theoretical description of their physical properties. Graphene is a two-dimensional material [1] which further belongs to the family of Dirac materials [2]. These materials have at least one common property. A great part of the underlying physics behind these materials is governed by the Dirac equation. Low-energy quasiparticles in graphene behave like massless relativistic fermions as they are described by the 2D Dirac equation. Graphene is thus a perfect playground for simulating relativistic quantum physics on the table-top experiments.

There exist multilayered derivatives of graphene. Especially, bilayer graphene enjoys a great deal of research interest because of its many interesting properties. Famous ones are superconducting twisted bilayer [3], anomalous quantum Hall effect [4] or energy gap which can be tuned by an external electric field [5]. In addition to pseudospin and valley polarization coming from graphene, the bilayer brings the layer degree of freedom to the game.

For better understanding of physical phenomena in graphene or bilayer graphene, it is necessary to deal with the 2D Dirac equation. Solvable models in this area usually rely on translational or rotational symmetry so that the evolution equation can be reduced to one dimension [6].

Electron transport sometimes requires transfer from one channel to another. Devices that suit this task are called couplers. We show that two non-interacting parallel graphene sheets can work as a coupler if they turn into AA bilayer in a restricted area. We denote this device as AA bilayer coupler. It is worth mentioning that the experimental implementation of a related AB bilayer coupler was already done in [7].

1 Model of AA bilayer coupler

The Hamiltonian that describes the physical model of a coupler is

$$\begin{gathered} H = \begin{pmatrix} H_0 & t\theta(R-r) \\ t\theta(R-r) & H_0 \end{pmatrix}, \\ H_0 = -i\left[\sigma_r\partial_r + \frac{1}{r}\sigma_\varphi\partial_\varphi\right],\ \sigma_r = \begin{pmatrix} 0 & \mathrm{e}^{-i\varphi} \\ \mathrm{e}^{i\varphi} & 0 \end{pmatrix},\ \sigma_\varphi = i\begin{pmatrix} 0 & -\mathrm{e}^{-i\varphi} \\ \mathrm{e}^{i\varphi} & 0 \end{pmatrix}. \end{gathered} \tag{1}$$

Where we have introduced a constant hopping parameter $t \in \mathbb{R}$ and a radius $R > 0$ of the AA bilayer graphene region. The ordering of the wavefunction is $\Psi = (\psi_{A1}, \psi_{B1}, \psi_{A2}, \psi_{B2})$ (sublattice A, B; layer $1, 2$). We would like to analyze the scattering of Dirac particles on a coupler. The first step is to solve the eigenvalue equation of H. A great simplification of this task is achieved by the following unitary transformation $U = \mathrm{e}^{i\frac{\pi}{4}\sigma_2} \otimes \mathbb{I}$

$$UHU^\dagger = \left(\begin{array}{c|c} H_0 + t\theta(R-r) & 0 \\ \hline 0 & H_0 - t\theta(R-r) \end{array}\right). \tag{2}$$

The eigenvalue equation $UHU^\dagger U\Psi = EU\Psi, U\Psi(r,\varphi) = (\psi(r,\varphi), \chi(r,\varphi))^T$ takes the form

$$\begin{pmatrix} H_0 + t\theta(R-r) & 0 \\ 0 & H_0 - t\theta(R-r) \end{pmatrix}\begin{pmatrix}\psi \\ \chi\end{pmatrix} = E\begin{pmatrix}\psi \\ \chi\end{pmatrix} \iff \begin{matrix} H_0\psi = [E - t\theta(R-r)]\psi \\ H_0\chi = [E + t\theta(R-r)]\chi. \end{matrix} \tag{3}$$

On the right-hand side, there are two 2D Dirac equations where the energy is shifted by a constant t at $r < R$. We focus on the equation for $\psi(r,\varphi)$ and make the ansatz $\psi(r,\varphi) = \mathrm{e}^{im\varphi}(\psi_A(r), i\mathrm{e}^{i\varphi}\psi_B(r))$[1]. By the action of H_0 given by (1) on this ansatz, we separate the variables r and φ and get the coupled equations in variable r only

$$\begin{aligned} \left(\partial_r + \frac{m+1}{r}\right)\psi_B(r) &= \big[E - t\theta(R-r)\big]\,\psi_A(r) \\ \left(-\partial_r + \frac{m}{r}\right)\psi_A(r) &= \big[E - t\theta(R-r)\big]\,\psi_B(r). \end{aligned} \tag{4}$$

Decoupling the equations provides us the Bessel equation for $\psi_A(r)$ component

$$\psi_A'' + \frac{1}{r}\psi_A' + \left[(E - t\theta(R-r))^2 - \frac{m^2}{r^2}\right]\psi_A = 0. \tag{5}$$

The solution is known in Bessel (J_m, Y_m) or Hankel $(H_m^{(1)}, H_m^{(2)})$ functions. Before that, it is necessary to distinguish the domains $r > R$ and $r < R$ due to the discontinuity of the step

[1] $m \in \mathbb{Z}$ is the quantum number related to the total angular momentum $J_3\psi = (-i\partial_\varphi + 1/2\sigma_3)\psi = (m + 1/2)\psi$.

function θ. In summary, the wavefunction is sum over all m's ($C_1^{(m)}, C_2^{(m)}, S_1^{(m)}, S_2^{(m)} \in \mathbb{C}$)

$$\psi(r,\varphi) = \begin{cases} \sum_{m=-\infty}^{+\infty} \mathrm{e}^{im\varphi} \left[C_1^{(m)} \begin{pmatrix} J_m(k_- r) \\ i\xi_- \mathrm{e}^{i\varphi} J_{m+1}(k_- r) \end{pmatrix} + C_2^{(m)} \begin{pmatrix} Y_m(k_- r) \\ i\xi_- \mathrm{e}^{i\varphi} Y_{m+1}(k_- r) \end{pmatrix} \right], & r < R \\ \sum_{m=-\infty}^{+\infty} \mathrm{e}^{im\varphi} \left[S_1^{(m)} \begin{pmatrix} H_m^{(1)}(kr) \\ i\xi \mathrm{e}^{i\varphi} H_{m+1}^{(1)}(kr) \end{pmatrix} + S_2^{(m)} \begin{pmatrix} H_m^{(2)}(kr) \\ i\xi \mathrm{e}^{i\varphi} H_{m+1}^{(2)}(kr) \end{pmatrix} \right], & r \geq R, \end{cases} \tag{6}$$

where we have defined $k = |E|, k_\pm = |E \pm t|, \xi = \mathrm{sgn}\,(E)\,, \xi_\pm = \mathrm{sgn}\,(E \pm t)$. The component $\psi_B(r)$ is calculated from the second line of (4) where we have used the recurrence $(-\partial_r + m/r)J_m(kr) = kJ_{m+1}(kr)$. We proceed analogously for χ. The wavefunction Ψ is recovered from $\Psi = U^\dagger(\psi, \chi)$. The regularity of Ψ in $r = 0$ forces us to discard the Bessel function Y_m due to its divergence $Y_m(0) = \pm\infty$. The explicit eigenfunctions of the coupler Hamiltonian, which will be further used in the text, can be written as ($\alpha = \pm 1$)

$$\Psi = \begin{cases} \sum_{m=-\infty}^{+\infty} i^m \mathrm{e}^{im\varphi} \left[C_1^{(m)} \begin{pmatrix} J_m(k_- r) \\ i\xi_- \mathrm{e}^{i\varphi} J_{m+1}(k_- r) \\ J_m(k_- r) \\ i\xi_- \mathrm{e}^{i\varphi} J_{m+1}(k_- r) \end{pmatrix} + C_2^{(m)} \begin{pmatrix} -J_m(k_+ r) \\ -i\xi_+ \mathrm{e}^{i\varphi} J_{m+1}(k_+ r) \\ J_m(k_+ r) \\ i\xi_+ \mathrm{e}^{i\varphi} J_{m+1}(k_+ r) \end{pmatrix} \right], & r < R \\ \sum_{m=-\infty}^{+\infty} i^m \mathrm{e}^{im\varphi} \left[\begin{pmatrix} J_m(kr) \\ i\xi \mathrm{e}^{i\varphi} J_{m+1}(kr) \\ 0 \\ 0 \end{pmatrix} + S_1^{(m)} \begin{pmatrix} H_m^{(\frac{3-\alpha}{2})}(kr) \\ i\xi \mathrm{e}^{i\varphi} H_{m+1}^{(\frac{3-\alpha}{2})}(kr) \\ 0 \\ 0 \end{pmatrix} + S_2^{(m)} \begin{pmatrix} 0 \\ 0 \\ H_m^{(\frac{3-\alpha}{2})}(kr) \\ i\xi \mathrm{e}^{i\varphi} H_{m+1}^{(\frac{3-\alpha}{2})}(kr) \end{pmatrix} \right], & r \geq R. \end{cases} \tag{7}$$

The scattering setup consists of an incoming plane wave Ψ_{in} which hits the AA bilayer region. After that, it is scattered in the form of a circular wave Ψ_{sc}. For the investigation of the coupling properties, we assume an incoming wave localized on the layer 1. The scattering states have to satisfy the asymptotical behavior for large r ($\alpha = \pm 1$)

$$\Psi_{in} + \Psi_{sc} \sim \frac{1}{\sqrt{2}} \begin{pmatrix} 1 \\ 1 \\ 0 \\ 0 \end{pmatrix} e^{i\xi kx} + \frac{1}{\sqrt{2}} \begin{pmatrix} f_E^{(A1)}(\varphi) \\ f_E^{(B1)}(\varphi) \\ f_E^{(A2)}(\varphi) \\ f_E^{(B2)}(\varphi) \end{pmatrix} \frac{e^{i\alpha kr}}{\sqrt{r}}. \tag{8}$$

We have already chosen the part $r \geq R$ of the wavefunction Ψ given by (7) such that it satisfies the asymptotics (8). This can be proven if we realize $\mathrm{e}^{ikx} = \sum_m i^m \mathrm{e}^{im\varphi} J_m(kr)$ and the asymptotical behavior of Hankel functions $H_m^{(\frac{3-\alpha}{2})}(kr) \overset{r\gg 1}{\sim} \sqrt{\frac{2}{rk\pi}} \mathrm{e}^{-i\alpha(m\pi/2+\pi/4)} \mathrm{e}^{i\alpha kr}$ [8]. Whether we take $\alpha = 1$ or $\alpha = -1$ depends on the sign of the radial probability current $\Psi_{sc}^\dagger \sigma_r \Psi_{sc}$. The scattered particles should propagate from the scattering region (not to) so the requirement $\Psi_{sc}^\dagger \sigma_r \Psi_{sc} > 0$ fully specifies α.

The scattering amplitudes $f_E^{(A1)}, \ldots, f_E^{(B2)}$ in (8) encode the angle dependence of the scattered wave, i.e. there could exist directions φ in which scattering takes place more prominently. However, the scattering amplitudes have yet unknown constants $C_{1,2}^{(m)}, S_{1,2}^{(m)}$. Those constants are uniquely determined by the requirement of continuity of Ψ in $r = R$, that is $\forall \varphi \in [0, 2\pi) : \lim_{r\to R^+} \Psi(r,\varphi) = \lim_{r\to R^-} \Psi(r,\varphi)$. The scattering amplitudes are

connected to experimentally measurable *differential cross section* $d\sigma^{(1,2)}/d\varphi$ for layer 1 and 2

$$\frac{\mathrm{d}\sigma^{(1)}}{\mathrm{d}\varphi} = \mathrm{Re}\left(f_E^{(A1)}\overline{f_E^{(B1)}}\mathrm{e}^{i\varphi}\right), \quad \frac{\mathrm{d}\sigma^{(2)}}{\mathrm{d}\varphi} = \mathrm{Re}\left(f_E^{(A2)}\overline{f_E^{(B2)}}\mathrm{e}^{i\varphi}\right). \tag{9}$$

The differential cross section is proportional to the probability that the Dirac fermions are scattered at the angle φ. Integrating over all angles gives us total cross section

$$\sigma^{(1,2)}(E) = \int_0^{2\pi} \frac{\mathrm{d}\sigma^{(1,2)}}{\mathrm{d}\varphi}\, d\varphi = \sum_{m=-\infty}^{+\infty} \sigma_m^{(1,2)}(E). \tag{10}$$

The elements $\sigma_m^{(1,2)}$ are called *partial cross sections*. They describe the scattering of particles with fixed angular momentum quantum number m. It corresponds to the scattering situation when we take the incoming wave as $\mathrm{e}^{im\varphi}(J_m(kr), i\xi\mathrm{e}^{i\varphi}J_{m+1}(kr), 0, 0)^T$ instead of $\mathrm{e}^{i\xi kx}(1,1,0,0)^T$.

2 Results and Discussion

The partial cross sections are shown in Fig. 1. As $\sigma_m^{(2)} \neq 0$, the incoming Dirac fermions from layer 1 can be transferred to layer 2. The values of $\sigma_m^{(2)}$ and $\sigma_m^{(1)}$ do not differ much,

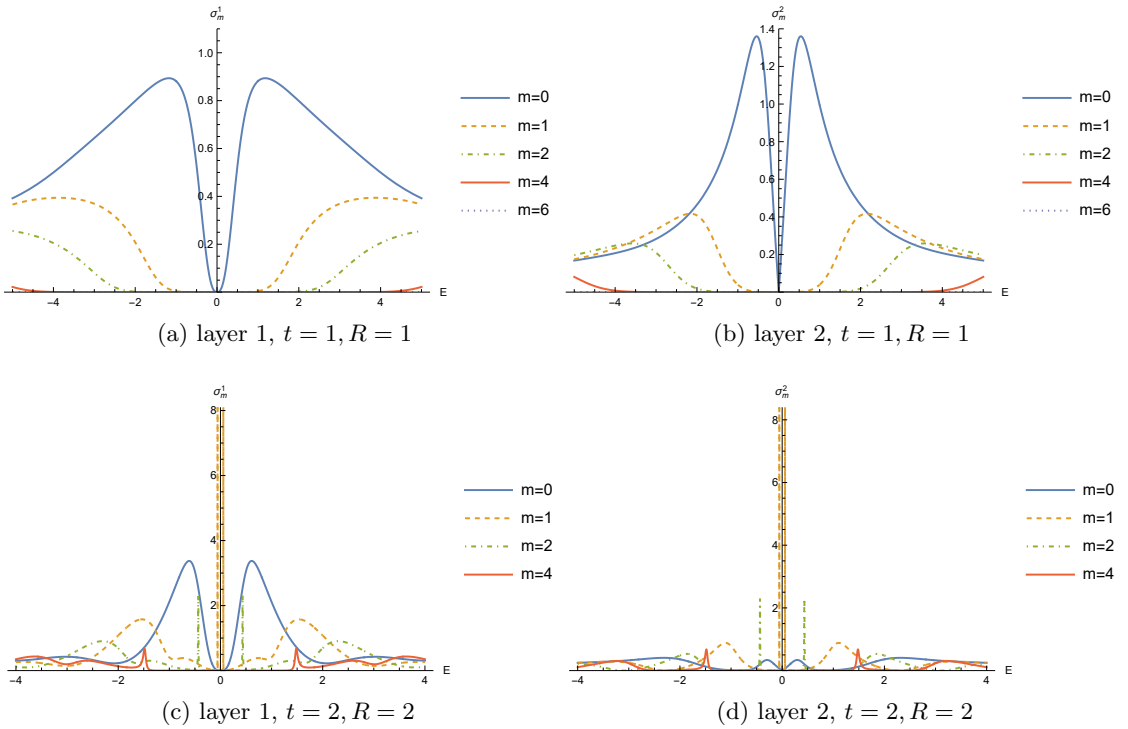

(a) layer 1, $t = 1, R = 1$ (b) layer 2, $t = 1, R = 1$

(c) layer 1, $t = 2, R = 2$ (d) layer 2, $t = 2, R = 2$

Figure 1: (*Color online*) The partial cross sections $\sigma_m^{(1,2)}(E)$ given by (10) plotted as a function of the incoming wave energy E. The radius R and hopping parameter t are below each figure.

so the transfer should not be highly inefficient. Both $\sigma_m^{(1)}$ and $\sigma_m^{(2)}$ exhibit peaks that point to the resonances of states with given m (quasi-bound states) inside the AA bilayer region. States with the energy of the peaks are trapped for a finite time in the AA bilayer region. Narrower peaks mean longer trapping time. Deeper analysis of the trapping time can be found in [9].

The peaks become narrower if we increase R (and thus the area) of AA bilayer or if we increase the strength of the coupling t. These increases cause a higher possibility of particle interaction with the scattering region. We can further observe that there exist energies for which, except for one specific m, all partial cross sections vanish. For example, it is state $m = 0$ and $E \approx 0.5$ in Fig. 1b or $m = 1$ and $E \approx 0.02$ in Fig. 1d. The scattering of states with a quantum number m on layer 2 does not take place if the corresponding $\sigma_m^{(2)}$ vanishes. Based on this observation, we can construct a filter that passes states with one selected m to layer 2.

From the differential cross sections in Fig. 2, it is evident that the scattering is strongly anisotropic. The absence of backscattering at the angle $\varphi = \pi$ can be useful because no

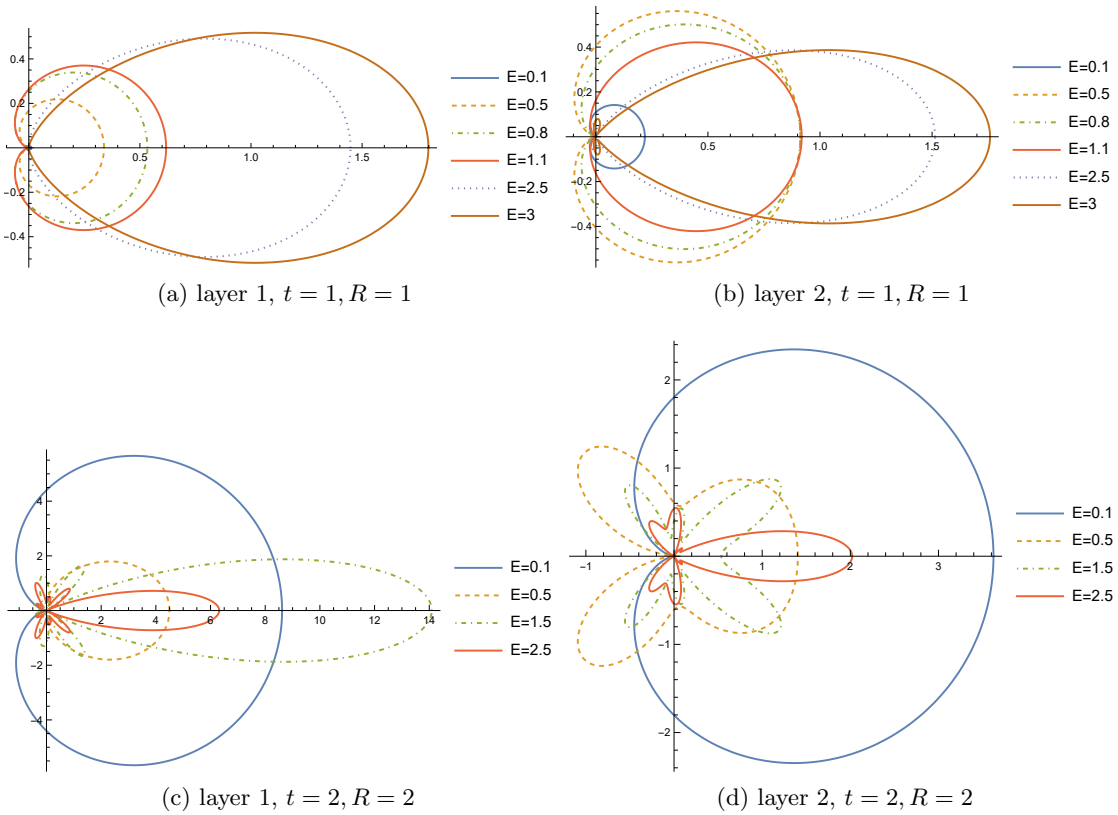

(a) layer 1, $t = 1, R = 1$

(b) layer 2, $t = 1, R = 1$

(c) layer 1, $t = 2, R = 2$

(d) layer 2, $t = 2, R = 2$

Figure 2: (*Color online*) The differential cross sections $d\sigma^{(1,2)}/d\varphi$ given by (9) plotted as polar graphs in variable φ.

particles return to the source that emits incoming Dirac fermions (in the form of plane waves). Let us summarize the most significant results obtained from the analysis of partial and differential cross sections:

1. The coupler can transfer incoming particles from layer 1 to layer 2.

2. There is no phenomenon in which the scattering on one layer somehow substantially outweighs the scattering on the other layer. If it did happen, it would be ineffective to transfer Dirac fermions between layers.
3. We are able to fully filter out the $m = 0$ state from an incoming plane wave on layer 2 (see Fig. 1b). Higher values of R and t allow us to separate states with higher m (state $m = 1$ in Fig. 1d).
4. Dirac fermions go mostly through the AA region in the direction $\varphi = 0$ (see Fig. 2). The absence of backscattering is also clearly visible there.
5. The peaks in the partial cross sections point to the formation of quasi-bound states in the coupling AA region.
6. The scattering pattern of low-energy fermions in layer 2 is robust to the change of R, t. This observation is based on the layer 2 blue line ($E = 0.1$) in Fig. 2 where the blue line retains the shape of the cardioid.

3 Conclusions

Our aim was to qualitatively analyze the scattering of Dirac particles on a solvable model called the AA bilayer coupler. The 2D scattering method is quite general and can also be used for AB or more exotic graphene bilayers. The 2D Dirac equation is not even limited to the physics of graphene but is valid for all 2D Dirac materials such as transition metal dichalcogenides[2]. To the originally intended proof of particle transfer between layers, we have discovered additional possibilities for the use of the coupler. In the future, we would like to study these in more complex physical conditions, e.g. in the presence of electric or magnetic fields.

References

[1] Mikhail I. Katsnelson. *The Physics of Graphene.* 2 edition. Cambridge University Press, 2020.

[2] Wehling, T.O. and Black-Schaffer, A.M. and Balatsky, A.V. Dirac materials. *Advances in Physics* **63**(1): 1-76, 2014.

[3] Yuan Cao, Valla Fatemi, Shiang Fang, Kenji Watanabe, Takashi Taniguchi, Efthimios Kaxiras, and Pablo Jarillo-Herrero. Unconventional superconductivity in magic-angle graphene superlattices. *Nature* **556**(7699): 43-50, 2018.

[4] Edward McCann and Vladimir I. Fal'ko. Landau-Level Degeneracy and Quantum Hall Effect in a Graphite Bilayer. *Physical Review Letters* **96**(8): 086805, 2006.

[5] Yuanbo Zhang, Tsung-Ta Tang, Caglar Girit, Zhao Hao, Michael C. Martin, Alex Zettl, Michael F. Crommie, Y. Ron Shen, and Feng Wang. Direct observation of a widely tunable bandgap in bilayer graphene. *Nature* **459**(7248): 820–823, 2009.

[6] Charles A. Downing and Mikhail E. Portnoi. Zero-Energy Vortices in Dirac Materials. *physica status solidi (b)* **256**(9): 1800584, 2019.

[2] They consist of chalcogen (S, Se, Te) and transition metals (Ti, V, Mo, Pd, Pt...), e.g. $MoS_2, WS_2, PtTe_2$.

[7] Yung-Chang Lin, Amane Motoyama, Pablo Solís-Fernández, Rika Matsumoto, Hiroki Ago, and Kazu Suenaga. Coupling and Decoupling of Bilayer Graphene Monitored by Electron Energy Loss Spectroscopy. *Nano Letters* **21**(24): 10386–10391, 2021.

[8] Milton Abramowitz and Irene A. Stegun. *Handbook of Mathematical Functions with Formulas, Graphs, and Mathematical Tables*. Dover, New York, ninth Dover printing, tenth GPO printing edition, 1964.

[9] Ş. Kuru, J. Negro, L.M. Nieto, and L. Sourrouille. Massive and massless twodimensional Dirac particles in electric quantum dots. *Physica E: Low-dimensional Systems and Nanostructures* 142:115312, 2022.

Acknowledgement

This work was supported by the Grant Agency of the Czech Technical University in Prague, grant No. SGS13/219/OHK4/3T/14, and Czech Science Foundation, grant No. 14-36566G.